Droplet formation of highly viscous newtonian and non-newtonian fluids in a microfluidic flow focusing device : scaling of droplet size and production frequency

C. Authesserre[*], F. Bottausci[*], G. Costa[*], M. Alessio[*], P.Y. Benhamou[**], B. Icard[*] and F. Rivera[*]

[*]CEA-LETI, MINATEC Campus, 17 avenue des Martyrs, 38054 Grenoble Cedex 9, France,
[**]Department of Endocrinology, Grenoble University Hospital, 38043 Grenoble, France
Contacts: claire.authesserre@cea.fr, florence.rivera@cea.fr

ABSTRACT

In this paper, we report for the first time the production of ~200 μm-size monodispersed droplets using highly viscous newtonian and non-newtonian fluids (up to 3.6Pa.s) in a pressure actuated device. Droplet size and production frequency have been characterized regarding flow rates and fluid properties (viscosity of the dispersed phase, interfacial tension, shear-thinning properties) and scaling laws are presented. Shear-thinning behavior results in smaller droplet size and higher production frequency than droplets produced with a newtonian fluid having the same zero-shear rate viscosity.

Keywords: microfluidics, flow-focusing device, droplet, high viscosity, non-newtonian, shear-thinning

1 INTRODUCTION

Polymer particles are largely used for different applications such as chromatography columns, calibration standards, drug delivery or cell encapsulation [1]. For all these applications, high size monodispersity and production frequency are required.

Microfluidics flow focusing devices (MFFD) allows the continuous production of monodispersed droplets. Droplet formation and break-up mechanism in MFFD have been extensively investigated using air or low viscosity newtonian fluids as dispersed phase (<0.1Pa.s) [2–4]. However, for many applications, polymers need to be used at high concentration and are therefore highly viscous and non-newtonian. Only few studies on MFFD report the use of high viscosity newtonian fluids (up to 1.8Pa.s) [1,3]. Non-newtonian behavior have been studied only for Boger fluids (fluids with constant viscosity over shear rate) [5,6].

Here, focusing on the dripping regime, we study the droplet formation of highly viscous (up to 3.6Pa.s) newtonian and non-newtonian polymers to understand the influence of the shear-thinning behavior.

First, rheological behavior of the dispersed phase solutions is investigated. Then, results on droplet volume and production frequency are presented with the obtained scaling laws.

2 MATERIAL AND METHODS

2.1 Microfluidic chip design and fabrication

A flow focusing design previously described [7] was used to produce droplets. Microfluidic chips were made of poly(dimethylsiloxane) (PDMS) using molds produced with common soft-lithography techniques. Chips were bonded on a glass slide using plasma O_2 treatment and then silanized to make hydrophobic channels. The channel height is h=200μm and the channel width is w=200μm.

2.2 Solutions and fluid characterization

Alginate and Ficoll® solutions were used as the dispersed phase (d). Alginate (Pronova SLG100, NovaMatrix) was prepared in deionized water containing 150mM NaCl and 25mM HEPES (pH=7.4) at concentration ranging from 1 to 3%wt/wt. Ficoll® (PM400, F8016, Sigma) was diluted in deionized water at concentration ranging from 0.5 to 1.2g/mL. Viscosity (η_d) and non-newtonian behavior of these solutions were characterized on a rheometer (Bohlin Gemini, Malvern) using a cone/plate geometry with a cone 1/60 (60mm in diameter, cone angle of 1°) and a plate equipped with a temperature control unit. Results are presented in section 3.

Super-refined soybean oil (Croda) was used as the continuous phase (c). The viscosity of this newtonian fluid is η_c=52mPa.s (Brookfield DVII+ Pro). Interfacial tension (σ) between the dispersed phase and the continuous phase was tuned adding Span80 (S6760, Sigma) to soybean oil. Interfacial tensions were respectively σ=21.1, 16.2, 14.2 and 8.3mN/m for 0, 0.15, 0.24, 0.35%v/v Span80 (Krüss DSA100).

All measurements were carried out at 22.5°C (room temperature).

2.3 Experimental setup

Fluids were motioned by regulated driving pressures delivered by micropumps (MFCS-8C 0-1000mbar, Fluigent). Experiments were visualized under a microscope (Olympus AX70, objective 5x) and image sequences were acquired using a high speed camera (Mikrotron GmbH, MotionBlitz Eosens), up to 1600 fps.

2.4 Flow characterization

Volumetric flow rate of the continuous phase (Q_c) was calculated using an analytical model of the microfluidic system, previously validated using experimental data (data not shown). Volumetric flow rate of the dispersed phase (Q_d) was determined doing the product of the production frequency f and the droplet volume V. In all experiments presented in this paper, Q_c was kept constant (Q_c=2.45mL/h) and Q_d ranged from 0mL/h to the maximal flow rate before jetting regime occurs.

2.5 Droplet characterization

Droplet diameter (D) was measured using ImageJ software. For D<h, the droplet volume (V) was calculated as V=(4/3)π(D/2). For D>h, the flattening of the droplet is taken into account and its volume was approximated using Nie's expression [2].

Droplet production frequency (f) was calculated using the number of images separating the break-up of two consecutive droplets and the frame rate of the camera.

3 DISPERSED PHASE RHEOLOGY

Viscosity and shear-thinning behavior of the dispersed phase were characterized (Table 1). Figure 1 shows that Ficoll® viscosity is quasi-constant over shear rate whereas alginate viscosity decreases when the shear rate increases, showing a shear-thinning behavior.
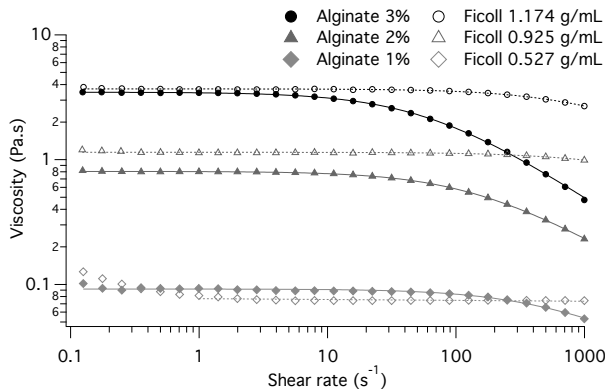

Figure 1: Viscosity of alginate and Ficoll® solutions versus shear rate. Markers correspond to experimental data and lines correspond to the Carreau-Yasuda model.

Different models have been proposed to describe the shear-thinning behavior of polymers. Here, data fitting is performed using the Carreau-Yasuda model in which fluids behave as a newtonian fluid at low shear rate ($\dot{\gamma} \ll 1/\tau$) and as a power-law fluid at high shear rate ($\dot{\gamma} \gg 1/\tau$). In this model, the viscosity follows the law:

$$\eta(\dot{\gamma}) = \eta_0 \left[1 + (\tau\dot{\gamma})^a \right]^{\frac{1-n}{a}} \qquad (1)$$

where η is the apparent viscosity, η_0 is the zero-shear rate viscosity, $\dot{\gamma}$ is the shear rate, τ is the relaxation time that sets the cross-over shear rate (λ), a is a constant that sets the size and shape of the cross-over region (a=1) and n is a dimensionless constant that characterizes the shear-thinning degree (n=1 for newtonian fluids and 0<n<1 for shear-thinning fluids).

Dispersed phase (d)	η_{0d} (mPa.s)	τ (s)	$\lambda=1/\tau$ (s^{-1})	n
Alginate 3% wt/wt	3480	0.0162	62	0.32
Alginate 2% wt/wt	806	0.0075	133	0.42
Alginate 1% wt/wt	92	0.0024	417	0.57
Ficoll® 1.174 g/mL	3693	0.0013	769	0.63
Ficoll® 0.925 g/mL	1147	0.0012	833	0.82
Ficoll® 0.527 g/mL	78	-	-	0.99

Table 1: Rheological properties of alginate and Ficoll® solutions. η_{0d} is the viscosity at zero-shear rate, τ is the characteristic relaxation time and n is a constant that characterizes the degree of shear-thinning.

While increasing polymer concentration, one can note that shear-thinning behavior increases (n decreases) and the cross-over shear rate decreases. For shear rates and concentrations used, alginate is non-newtonian (n<0.6) whereas Ficoll® exhibits only a slight shear-thinning behavior for the highest concentration. The constant n and the cross-over shear rate λ are significantly lower for alginate than for Ficoll®, suggesting that this latter is a good candidate to study the influence of shear-thinning behavior on droplet formation of highly viscous fluids.

4 DROPLET SIZE VS FLOW RATE RATIO

Figure 2 and Figure 3 show that droplet volume scales with the flow rate ratio as a power law. Moreover, at a fixed Q_d/Q_c, droplet volume increases when dispersed phase viscosity or interfacial tension increases (see section 6).

Figure 2 shows two distinct domains. The change occurs at a critical volume V_{cr}=8.2x$10^{-11}m^3$ ($Q_d/Q_c \approx 0.3$) corresponding to D=250µm, the nozzle width. For D>250µm, droplet volume seems to be linearly proportional to Q_d/Q_c (α=1). This is in accordance with results from Garstecki et al. [8] for air droplet in oil, meaning that in this domain droplet formation probably results from a geometry-controlled breakup mechanism. For D<250um, droplet volume scales with Q_d/Q_c as a power law with a power 0<α<0.5 (see equation 2) depending on η_d (see inset in Figure 2). This suggests a shear-rate-controlled breakup mechanism. When η_d increases, the dependence of the volume on the flow rate ratio becomes weaker. Results show that such type of dependancy, previously described for low viscosity newtonian fluids [2,9], can also be applied for highly viscous newtonian and non-newtonian fluids.
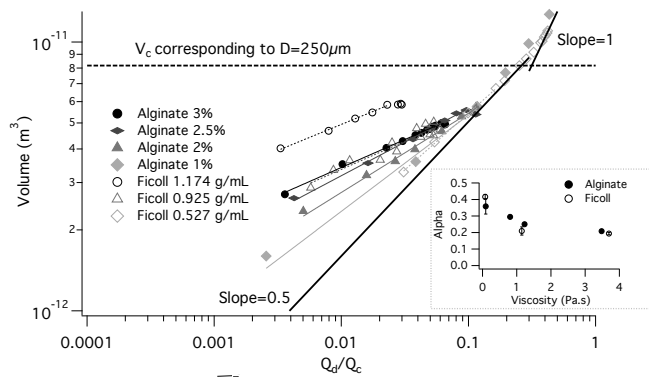
Figure 2: Droplet volume versus flow rate ratio: influence of the dispersed phase viscosity. σ is kept constant at σ=21.1mN/m using pure soybean oil as the continuous phase.

Figure 3 also shows two distinct domains. For Q_d/Q_c <0.02, σ significantly influences the droplet volume, suggesting a capillary-controlled breakup mechanism. The coefficient of the power law V_0 (see equation 2) is influenced by σ (see inset in Figure 3). For Q_d/Q_c>0.02, it seems that droplet volume is less influenced by σ. This could be explained by the fact that for these flow rate ratios, shear stresses increase and become more important than interfacial tension, in accordance with the shear-rate controlled domain in Figure 2.
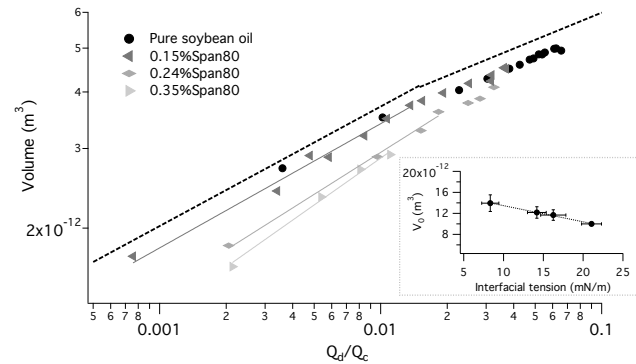

Figure 3: Droplet volume versus flow rate ratio: influence of interfacial tension. η_d is kept constant using 3%wt/wt alginate as the dispersed phase.

To summarize, we find that when flow rate ratio increases, droplet breakup is progressively controlled by the interfacial tension (Q_d/Q_c<0.02), the shear stress (0.02<Q_d/Q_c<0.3) and then the geometry of the MFFD (Q_d/Q_c>0.3). Moreover, we find that droplet volume follows the relation:

$$V \propto V_0 \left(\frac{Q_d}{Q_c} \right)^{\alpha} \qquad (2)$$

where $V_0(\sigma)$ and $0 < \alpha(\eta_d) < 0.5$ for Q_d/Q_c <0.3 and $\alpha \approx 1$ for Q_d/Q_c >0.3.
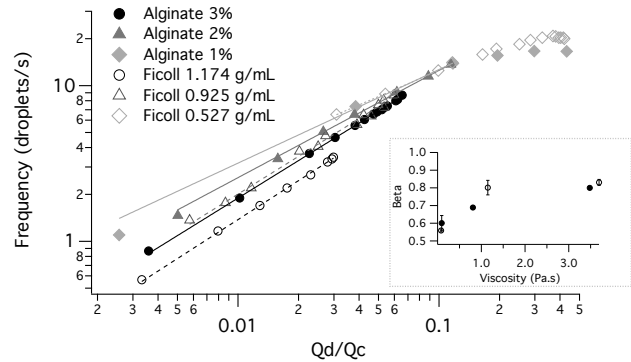
5 DROPLET PRODUCTION FREQUENCY VS FLOW RATE RATIO

Figure 4: Droplet production frequency versus flow rate ratio: influence of the dispersed phase viscosity. σ is kept constant at σ=21.1mN/m using pure soybean oil as the continuous phase.
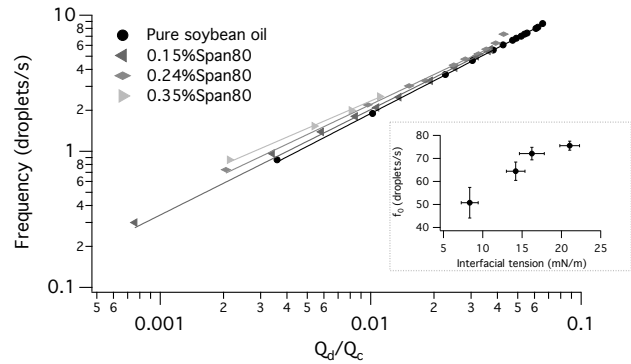

Figure 5: Droplet production frequency versus flow rate ratio: influence of the interfacial tension. η_d is kept constant using 3%wt/wt alginate as the dispersed phase.

Figure 4 shows that when the flow rate ratio increases, droplet frequency increases until a critical flow rate ratio Q_d/Q_c=0.2 where droplet frequency becomes constant. This is in accordance with the two domains observed in Figure 2. When Q_d/Q_c>0.2-0.3, as droplet volume rapidly increases with Q_d/Q_c, frequency stops increasing to satisfy mass conservation during breakup. For Q_d/Q_c<0.2, droplet production frequency scales with the flow rate ratio as a power law, with a power 0.5<β<1 depending on viscosity (see inset in Figure 4). Figure 5 shows that σ slightly influences the production frequency. That is the coefficient of the power law f_0 (see equation 3) which is influenced by σ (see inset in Figure 5). At fixed Q_d/Q_c, frequency increases when η_{0d} and σ decrease (see section 6).

To summarize, we find that droplet volume follows the relation:

$$f \propto f_0 \left(\frac{Q_d}{Q_c} \right)^{\beta} \qquad (3)$$

where $f_0(\sigma)$ and $0.5 < \beta(\eta_d) < 1$

6 INFLUENCE OF FLUID PROPERTIES AT FIXED FLOW RATE RATIO

At fixed Q_d/Q_c, droplet volume and production frequency respectively increases and decreases when η_{0d} increases (see Figure 6). Moreover, for same η_{0d}, alginate droplets are smaller than Ficoll droplets and are produced with a higher frequency. This means that alginate has a lower apparent viscosity than Ficoll during droplet formation. The volume and frequency differences between alginate and Ficoll increase when η_{0d} increases. This is in accordance with the shear-thinning behavior of alginate and the results presented in section 3 where it has been shown that the difference in shear-thinning degree between alginate and Ficoll increases with increasing η_{0d}. We show here that the shear-thinning behavior of the polymers therefore facilitates the droplet formation of highly viscous fluids.
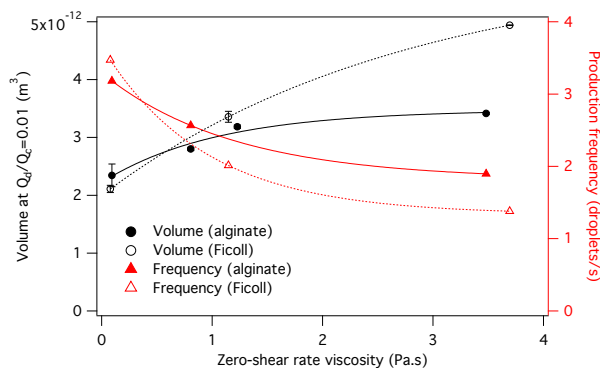

Figure 6: Influence of fluid properties on droplet volume and production frequency at $Q_d/Q_c=0.01$

At fixed Q_d/Q_c, droplet volume and production frequency respectively increases and decreases when σ increases (Figure 7). For a given dispersed phase and flow rate ratio, droplet production frequency can therefore be maximized using a low interfacial tension between the dispersed phase and the continuous phase.
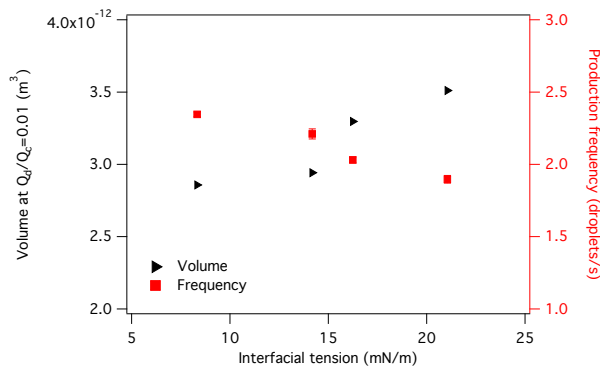

Figure 7: Influence of interfacial tension on droplet volume and production frequency at $Q_d/Q_c=0.01$

7 CONCLUSION

In this paper, we characterize for the first time the droplet formation of both newtonian and non-newtonian polymers with a viscosity up to 3.6 Pa.s, showing that shear-thinning behavior results in smaller droplet size and higher production frequency.

The defined scaling laws will be helpful for the future development of microfluidic droplet generation systems, in particular to optimize the production frequency.

REFERENCES

[1] Z. Nie, S. Xu, M. Seo, P. C. Lewis, and E. Kumacheva, "Polymer particles with various shapes and morphologies produced in continuous microfluidic reactors," *J. Am. Chem. Soc.*, vol. 127, no. 22, pp. 8058–8063, 2005.

[2] Z. Nie, M. Seo, S. Xu, P. C. Lewis, M. Mok, E. Kumacheva, G. M. Whitesides, P. Garstecki, and H. a. Stone, "Emulsification in a microfluidic flow-focusing device: Effect of the viscosities of the liquids," *Microfluid. Nanofluidics*, vol. 5, pp. 585–594, 2008.

[3] T. Cubaud and T. G. Mason, "Capillary threads and viscous droplets in square microchannels," *Phys. Fluids*, vol. 20, no. 5, 2008.

[4] W. Lee, L. M. Walker, and S. L. Anna, "Role of geometry and fluid properties in droplet and thread formation processes in planar flow focusing," *Phys. Fluids*, vol. 21, no. 2009, 2009.

[5] B. Steinhaus, A. Q. Shen, and R. Sureshkumar, "Dynamics of viscoelastic fluid filaments in microfluidic devices," *Phys. Fluids*, vol. 19, no. 7, 2007.

[6] P. E. Arratia, J. P. Gollub, and D. J. Durian, "Polymeric filament thinning and breakup in microchannels," *Phys. Rev. E - Stat. Nonlinear, Soft Matter Phys.*, vol. 77, pp. 1–6, 2008.

[7] J. Berthier, S. Le Vot, P. Tiquet, N. David, D. Lauro, P. Y. Benhamou, and F. Rivera, "Highly viscous fluids in pressure actuated flow focusing devices," *Sensors Actuators A Phys.*, vol. 158, no. 1, pp. 140–148, Mar. 2010.

[8] P. Garstecki, H. a. Stone, and G. M. Whitesides, "Mechanism for flow-rate controlled breakup in confined geometries: A route to monodisperse emulsions," *Phys. Rev. Lett.*, vol. 94, no. April, pp. 1–4, 2005.

[9] T. Ward, M. Faivre, M. Abkarian, and H. a. Stone, "Microfluidic flow focusing: Drop size and scaling in pressure versus flow-rate-driven pumping," *Electrophoresis*, vol. 26, no. 19, pp. 3716–3724, 2005.